EARTH SURFACE PROCESSES AND LANDFORMS
Earth Surf. Process. Landforms (2016)

Published online in Wiley Online Library
(wileyonlinelibrary.com) DOI: 10.1002/esp.3996

Spillage sedimentation on large river floodplains

John Lewin,[1] Philip J. Ashworth[2]* and Robert J. P. Strick[2]
[1] Department of Geography and Earth Sciences, Aberystwyth University, Llandinam Building, Penglais, Aberystwyth, SY23 3DB, UK
[2] Division of Geography and Geology, School of Environment and Technology, University of Brighton, Brighton, Sussex, BN2 4GJ, UK

Received 1 December 2015; Revised 20 May 2016; Accepted 13 June 2016

*Correspondence to: Philip Ashworth, Division of Geography and Geology, School of Environment and Technology, University of Brighton, Brighton, Sussex, BN2 4GJ, UK. E-mail: p.ashworth@brighton.ac.uk

ESPL
Earth Surface Processes and Landforms

ABSTRACT: Active deposition across the floodplains of large rivers arises through a variety of processes; collectively these are here termed 'spillage sedimentation'. Three groups of 11 spillage sedimentation styles are identified and their formative processes described. Form presences on large river floodplains show different combinations of active spillage styles. Only some large floodplains have prominent levees; some have coarse splays; many have accessory channel dispersion and reworking, while still-water sedimentation in lacustrine environments dominates some lower reaches. Infills are also commonly funnelled into prior, and often linear, negative relief forms relating to former migration within the mainstream channel belt.

Shuttle Radar Topography Mission (SRTM) and Landsat 8 data are used to map spillage form types and coverage along a 1700 km reach of the Amazon that has an active floodplain width of up to 110 km with a systematic character transformation down-valley. Spillage forms associated directly with mainstream processes rarely account for more than 5% of the floodplain deposits. There is a marked decrease in floodplain point bar complexes (PBC) over 1700 km downstream (from 34% to 5%), and an increase in the prevalence of large water bodies (2% to 37%) and accompanying internal crevasses and deltas (0% to 5%). Spillage sedimentation is likely within the negative relief associated with these forms, depending on mainstream sediment-laden floodwater inputs.

Spillage style dominance depends on the balance between sediment loadings, hydrological sequencing, and morphological opportunity. Down-river form sequences are likely to follow gradient change, prior up-river sediment sequestration and the altered nature of spilled loads, but also crucially, local floodplain relief and incident water levels and velocities at spillage times. Considering style distribution quantitatively, as a spatially distributed set of identifiable forms, emphasizes the global variety to spillage phenomena along and between large rivers. © 2016 The Authors. Earth Surface Processes and Landforms published by John Wiley & Sons Ltd.

KEYWORDS: floodplain; spillage; overbank sedimentation; large rivers; Amazon River

Introduction

The world's largest rivers and their floodplains drain a significant proportion of the earth surface (Fielding *et al.*, 2012, their Figure 3) with modern terrestrial sedimentary basins covering ~16% of the current continental area excluding passive margin settings (Nyberg and Howell, 2015). These are major global sinks for sediments, nutrients, organics and pollutants (Allison *et al.*, 1998; Aufdenkamp *et al.*, 2011; Syvitski *et al.*, 2012). Despite recent advances in quantifying large river dynamics (Nicholas, 2013; Schuurman *et al.*, 2013) and describing channel patterning (Latrubesse, 2008; Ashworth and Lewin, 2012), much less progress has been made on understanding the diversity and deposits of the largest river floodplains (Dunne and Aalto, 2013) and detailed descriptions on the floodplain architectures and facies models 'are not yet viable' (Latrubesse, 2015). These 'large' river floodplains are here defined as the zone stretching up to 100 km in width that borders large rivers, themselves typically greater than 1 km wide, and composed of multiple and complex negative relief assemblages that are intermittently flooded (Lewin and Ashworth, 2014a). While the area of floodplain inundated in catastrophic floods may be extensive, and includes new avulsed courses beyond the current elevated channel, this flooding may only constitute a limited proportion of some very extensive alluvial spreads (Syvitski and Brackenridge, 2013), and floodwaters may rarely return to the main channel when spread across a large megafan surface (Weissmann *et al.*, 2015, their figure 18).

Large floodplains are rarely passive recipients of diffuse overbank sediments across tabular relief (Scown *et al.*, 2015). Instead, large river floodplains have an intricate 'depositional web' (Day *et al.*, 2008) with an array of linked depressions and channels that may both span and connect significant expanses of ponded water (Assine and Soares, 2004; Bonnet *et al.*, 2008; Trigg *et al.*, 2012; Lewin and Ashworth, 2014a). Deposition in and beyond this undulating topography takes a variety of forms. The range of out-of-channel sedimentation processes alongside larger rivers may collectively be characterized as *spillage phenomena* (Figure 1), active at flood-stage, and particularly, but not exclusively, bordering main channels or channel belts raised above valley floor level to create strong lateral elevation contrasts (Assine *et al.*, 2014). This may arise because of relatively narrow channel belt aggradation within wider valley floors, or because main-channel sedimentation

Figure 1. Spillage sedimentation on the Amazon at the peak of the annual hydrograph. The dashed white line delimits the water's edge of the main channel at the trough of the annual hydrograph on 24 December 2014. Note the differentiated forms of 'spillage' that contribute to floodplain construction and aggradation that are described in Table I and Figure 2. Satellite data available from the US Geological Survey and image dated 18 June 2015.

has only partially occupied larger subsiding basins or drowned Pleistocene valley forms excavated in relation to lower base levels. The troughs occupied by the low-gradient lower reaches of most large rivers reflect forms inherited from long histories that still are present at floodplain levels as well as in elevated terraces or buried sediments (Latrubesse, 2015). Flood-prone realms include long-standing lake-filled depressions and linear forms left by past river migration. By contrast, spillage sedimentation is less characteristic of large, radial, distributive fluvial systems (or 'DFS' as termed by Hartley *et al.*, 2010; Weissmann *et al.*, 2010) that are commonly found in foreland basins and build through a sequence of mostly in-channel depositional lobes as anabranches migrate back and forth across a megafan surface (Weissmann *et al.*, 2015).

The sequential process of sedimenting extensive channel-side negative relief (Lewin and Ashworth, 2014a) can be both varied and active without the intervention of main channel shifting. Palaeochannels deprived of their former mainstream flow discharges, and lateral accretion swales also cover the ground in part, and these direct later overbank processes. Equally, floodplain heterogeneity of forms and near-surface sediments can have feedback constraints on, and opportunities for, channel mobility by creating extra diversion potential at points of lower bank profiles linking to the relief beyond (Ashworth and Lewin, 2012). They can also form impediments to channel migration as strings of less erodible sediment 'plugs' (Schwendel *et al.*, 2015).

Here we consider current spillage phenomena, on a metre to multi-kilometre scale, along large rivers as a holistic class, but one involving 11 sub-groups of process-related forms. The objective is to initiate discussion of the striking global variety of large-river spillage sedimentation, and the worldwide geographies of spillage elements. Rather than focusing on one or other of the process groups as historically identified, and almost entirely examined in case studies (e.g. levees or crevasse splays at particular sites), spillage is treated as a complex process class so as to map all the activities visible on imagery that indicate the spatial presences and absences of process groups.

This paper is organized to: (i) describe the types, modes and diversity of spillage sedimentation on large river floodplains; (ii) illustrate the prevalence of spillage sedimentation styles along the world's largest river; (iii) consider the global presences of spillage phenomena on large rivers in general; and (iv) explain the combined roles of both active hydro-morphological processes and inherited forms in determining spillage sedimentation types and their preservation.

Spillage forms

Spillage styles may be sorted into three groups and 11 sub-types. The 11 identified here, broadly following previous studies of individual features (cf. Fryirs and Brierley, 2013; Wheaton *et al.*, 2015, their Table 4), are given in Table I together with listings of previous research on each type. They are also presented in diagram form in Figure 2 together with the codes adopted in this paper.

Floodplain and spillage deposition

Deposition from spilled sediment at flood stage occurs in three broad circumstances. As on smaller streams (Lewin and Hughes, 1980), there can be a systematic and sequential set of relationships between inundation extent and floodplain morphology showing hysteretic relationships with mainstream flood stage. At first, extra-channel flow deceleration may lead to near-mainstream deposition especially of coarser material. Secondly, as floodplains fill, negative relief elements may continue to channel sediment-laden water for longer distances. This may be via accessory channels, by backing up tributaries which themselves may also be independently feeding in sediment, and via new channels actively created by crevasse flow. Finally, a variety of inherited forms, many of long-standing, may guide and pond water; this ponded water may give near still-water sedimentation of fines over longer periods. Floodplain water bodies, with different and mostly lesser sediment content, may also be present quasi-independently through groundwater rise, local precipitation, and tributary input (Mertes, 1997). Thus mainstream spillage may be into lacustrine environments, or is even buffered against entry flow by already-high water levels (Lewin and Ashworth, 2014a). Floodplain water levels finally recede through evaporation, water table lowering, and return flows to the main channel where waning flow may also lead to channel margin deposition of residually transported fines. In totality, spillage sedimentation may broadly occur in these three broad domain groupings.

Sedimentation at main channel margins

The first grouping consists of deposits adjacent to major channels. These range from those dispersed only short distances in rapidly overflowing water as levees (MSa) and discrete bank

Table I. Classification scheme for spillage forms on large river floodplains (MS and SL) and the filling of previously formed floodplain topography (PF)

Spillages	Sub-type	Previous work
MS Mainstream sediments	a. Levees	Smith, 1986; Cazanacli and Smith, 1998; Brierley et al., 1997; Ferguson and Brierley, 1999; Saucier, 1994; Adams et al., 2004; Klasz et al., 2014; Aalto et al., 2008; Park and Latrubesse, 2015
	b. Bank-top splays	Coleman, 1969; Alexander et al., 1999; Van de Lagerweg et al., 2013; Shen et al., 2015
	c. Channel bars and islands	Bristow, 1987; Gurnell et al., 2001; Mardhiah et al. 2015; Rozo et al., 2014; Wintenberger et al., 2015
SL Secondary linear systems	d. Accessory channels	Dunne et al., 1998; Lewin and Ashworth, 2014a; Lewin and Ashworth, 2014b; Latrubesse, 2015
	e. Crevasse splays	O'Brien and Wells, 1986; Smith et al., 1989; Smith and Pérez-Arlucea, 1994; Bristow et al., 1999; Farrell, 2001; Toonen et al., 2016
	f. Crevasses with deltas	Bogen, 1982; Tye and Coleman, 1989; Latrubesse and Franzinelli, 2002; Rowland et al., 2010; Olariu et al., 2012
	g. Drainage nets	Day et al., 2008; Trigg et al., 2012; Lewin and Ashworth, 2014b
PF Prior-form following	h. Cutoff and palaeochannel fills	Dieras et al., 2013; Toonen et al., 2012; Constantine et al., 2014
	i. Ponded lake filling	Paira and Drago, 2007; Bonnet et al., 2008; Citterio and Piégay, 2009; Maurice Bourgoin et al., 2005, 2007; Latrubesse, 2012
	j. Point bar swales and chutes (inter-scroll bars)	Hickin and Nanson, 1975; Latrubesse and Franzinelli, 2002; Grenfell et al., 2012, 2014; Rozo et al., 2014; Harrison et al., 2015
	k. Diffuse overbank spreads	James, 1985; Pizzuto, 1987; Allison et al., 1998; Törnqvist and Bridge, 2002; Benedetti, 2003; Aalto et al., 2003, 2008

top splays of well sorted, coarser material (MSb), to channel margin slackwater deposits and waning-flow forms on top of bedforms and islands initiated during earlier flood flow peaks (MSc). Island growth by spillage is facilitated by vegetation development on non-migrating bars (Latrubesse, 2015), with sedimentation in flows that have become partly disconnected and may have been deflected by woody vegetation (Mardhiah *et al.*, 2015; Wintenberger *et al.*, 2015). The Mekong has particularly prominent levees, but also finer sediment accreting as channel-side ramps between set back levees that rise up to 15 m above bed level (Wood *et al.*, 2008). Elsewhere, where sedimentation rates have been measured beyond channel belts (Törnqvist and Bridge, 2002) and across levees (Aalto *et al.*, 2008), they drop off quite sharply away from the channel. In braided systems and meandering ones where there is lateral channel movement, material may continue to deposit in patches (Bätz *et al.*, 2015), or river migration may largely re-erode such material returning it to the channel in the short or medium term. Not only is levee identification difficult in the rock record (Brierley *et al.*, 1997), but present distributions along large rivers are also geographically restricted.

Isolated bank-top patches of coarser material commonly occur on braided and to a lesser extent on meandering channel systems (Ritter, 1975; Ferguson and Werritty 1983). Figure 3 (A) shows a reach of the braided Zambezi River with active sedimentation in the form of bar-top splays (MSb) at the barheads. Figure 4(A) and (B) shows a reach of the Jamuna (Brahmaputra) before and after a single monsoon season. The channel has been transformed, with a kilometre of bank recession, new migrating bars, and trimmed islands. But there is also a prominent overbank splay in part being funnelled into a prior palaeochannel (labelled MSb in Figure 4(B)). Figure 3(B) shows freshly deposited sediment on a bend of the Mississippi after the extreme floods of 1993 (see also Gomez *et al.*, 1997). Material has been dumped on the outer bend in levee-like form, but also across the inner point bar, funnelling between the lateral accretion ridges previously produced during point bar growth. Chute development upstream (natural or artificial), in this case as in others (Zinger *et al.*, 2011), may have injected an abnormal volume of eroded floodplain sediment that is then transferred out of channel. Elsewhere in the Mississippi delta system, overbank fine sedimentation has been shown to be episodic over centennial to millennial timescales, with high rates for a while, but then switching to alternative sites (Shen *et al.*, 2015). The authors relate this to autogenic control. This arises from elevation build up so that sedimentation shifts in location to alternative sites that by contrast may have undergone lowering by compaction.

Sedimentation in secondary linear systems

A second grouping involves secondary linear dispersion of sediments further away from main channels into what may be called the perirheic zone (Mertes, 1997). This may be via quasi-independent secondary channels (SLd, see Figure 3(D)) generally carrying finer sediment (Lewin and Ashworth, 2014a), with some developing scroll bars of their own (Rozo *et al.*, 2014). Others are shorter crevasse channels that either have subaerial splays (SLe), or sedimentation in standing water via channelized flows to create positive features such as deltas and linear subaqueous channels across shallow lakes (SLf). Some crevasses may be precursors to avulsion (Slingerland and Smith, 2004), but many exist for multiple seasons injecting mixed sediment loads for several kilometres across normally dry floodplains. Chen *et al.* (2011) reported 313 historically recorded breaches in artificially raised levees on the super-elevated Yellow River in a 300 year period. Waters and sediment may spread via low bank points without main channel banks being fully overtopped except in the most extreme events (Hudson *et al.*, 2013). Tributary channels may also significantly spread main channel sediment through the reversed flows that back up them from main rivers (Day *et al.*, 2008).

Where unconstrained, subaerial splays may involve migration of radiating channels and fan-like forms; loads may also disperse in deltaic features following deceleration in lacustrine

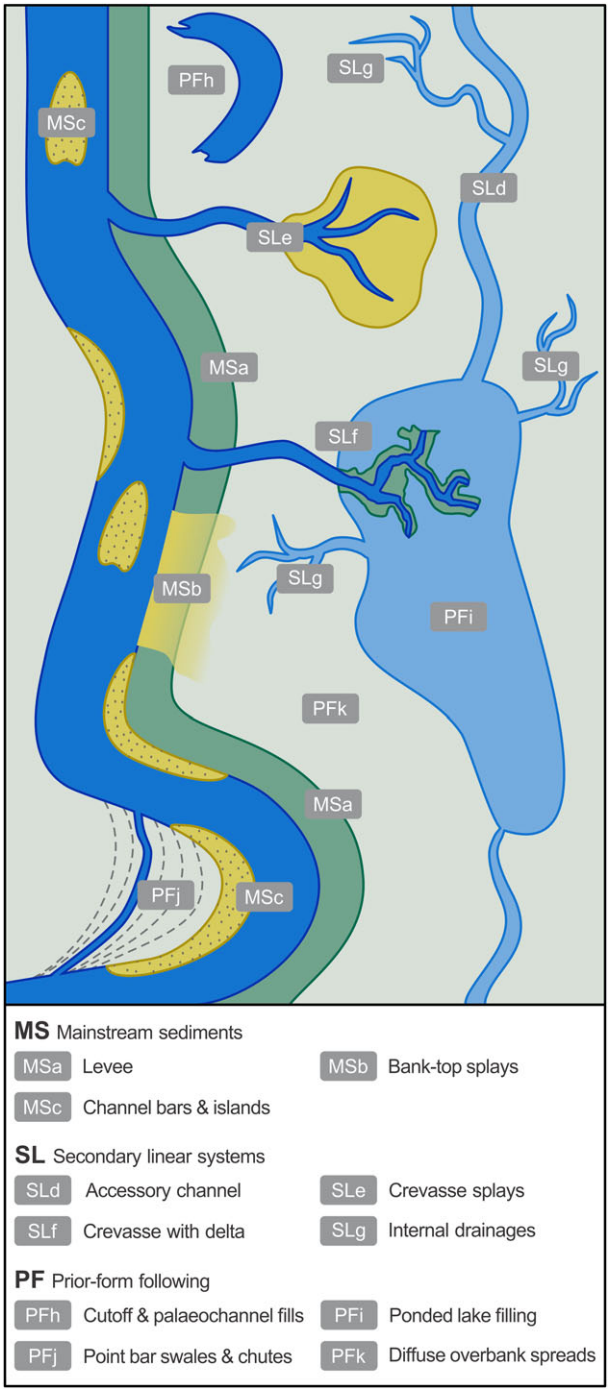

Figure 2. A spillage type model for large river floodplains. See also Table I.

environments. Here there may be a co-existing hierarchy of bifurcations, delta foresets and subaqueous levees (see Kleinhans *et al.*, 2013 for a review and discussion of contrasting bifurcations in fans and deltas). Splay deposits may spread across wetlands, extending and evolving their morphology to guide later infilling (Toonen *et al.*, 2016). Figure 3(C) shows an example of the kind that occurs along larger rivers where there are extensive water bodies and wetlands in subsiding basins or where main channel lateral sedimentation is restricted within what Syvitski *et al.* (2012) call 'container valleys'.

Prior forms, relicts from earlier processes, may pond rather than drain floodwaters, so that a range of tie channels (Day *et al.*, 2008) or chains of connector channels may erosively develop to link them. They may also extend erosively as dendritic networks draining surface waters or groundwaters (SLg). These convey sediment as much as contain them, producing elongate deposits in lakes (Rowland *et al.*, 2009, 2010 and see Figure 1), though such channels may also silt up where not flushed by exiting mainstream flows (Rowland *et al.*, 2005; Trigg *et al.*, 2012).

Prior-form following sedimentation

A third and final grouping of spillage sedimentation occurs broadly without independent topographic expression: infilling prior forms set by abandoned channels (PFh), as diffuse lake sedimentation (PFi), infilling the swales and related voids left during previous channel migration (PFj) and as indistinguishable diffuse spreads following the form of prior topography (PFk). The last have been modelled particularly in terms of an exponential decline in sedimentation rate with distance from the channel (James, 1985; Pizzuto, 1987), but the detail of floodplain topography complicates such relationships in practice (Trigg *et al.*, 2012; Harrison *et al.*, 2015), while such detail also affects the morphological development of linear splay forms (Toonen *et al.*, 2016).

Abandoned channel arms connected to mainstream flow may transfer sediment to infill forms such as meander cutoffs (oxbows), relict channels left after avulsion, or formerly active branches of anastomosing or braided rivers (Džubáková *et al.*, 2015). Constantine *et al.* (2010) have shown how the abandoned arm/active channel angle may be critical in allowing the old channel to be plugged with bedload and for sediment to accumulate in the old channel beyond. Neck cutoffs have generally higher angles and develop proximal-end plugs. Their oxbows may remain as open ponds longer than with chute cutoffs. At the other end of the scale, in braiding systems, bed material may continue to spill into and then to choke channels longitudinally along braid branches (Lewin and Ashworth, 2014a).

Point sedimentation on large rivers may evolve to give fills through spillage into negative relief in different ways. Figure 4 (C)–(F) shows two alternatives: (C) and (D) show swales between point bar ridges being infilled in a conventional manner; but (E) and (F) show a 'bifurcate bend' (Grenfell *et al.*, 2012). Here lateral migration of a bend has been followed by the formation of a sequential set of mid-channel bars with linear void 'channels' between (labelled PFh). These are being infilled by spillage, both blocking off the linear depressions from upstream (much as meander cutoffs may be plugged at the upstream end) and also extending into and narrowing them. In other cases, chute dissection of the point sediments once in place has been documented (Grenfell *et al.*, 2012, 2014). 'Point bar' relief on large rivers is not necessarily created by ridge and swale growth simply by attachment one by one at the inner bank margin, but also by island attachment (cf. Rozo *et al.*, 2014) and later stage excavation.

Lacustrine sedimentation rates are difficult to estimate meaningfully for the diverse settings and lake sizes associated with the floodplain of large rivers (Paira and Drago, 2007). Drago (2007) reports average sedimentation rates in the El Tigre Lake (31° 41'S, 60° 40'W) adjacent to the Rio Paraná of 32 g m^2 d^{-1} over a two year period with between 80 and 99% composed of inorganic material. Maurice-Bourgoin *et al.* (2007) suggest for the Amazon an average of 1.6 mm $yr.^{-1}$ (+/− 23%). These are data for individual lakes on large rivers and therefore may not be widely representative.

Anthropogenic transformations

All the above groups are grossly affected by anthropogenic activity. Major global rivers have been engineered for hundreds

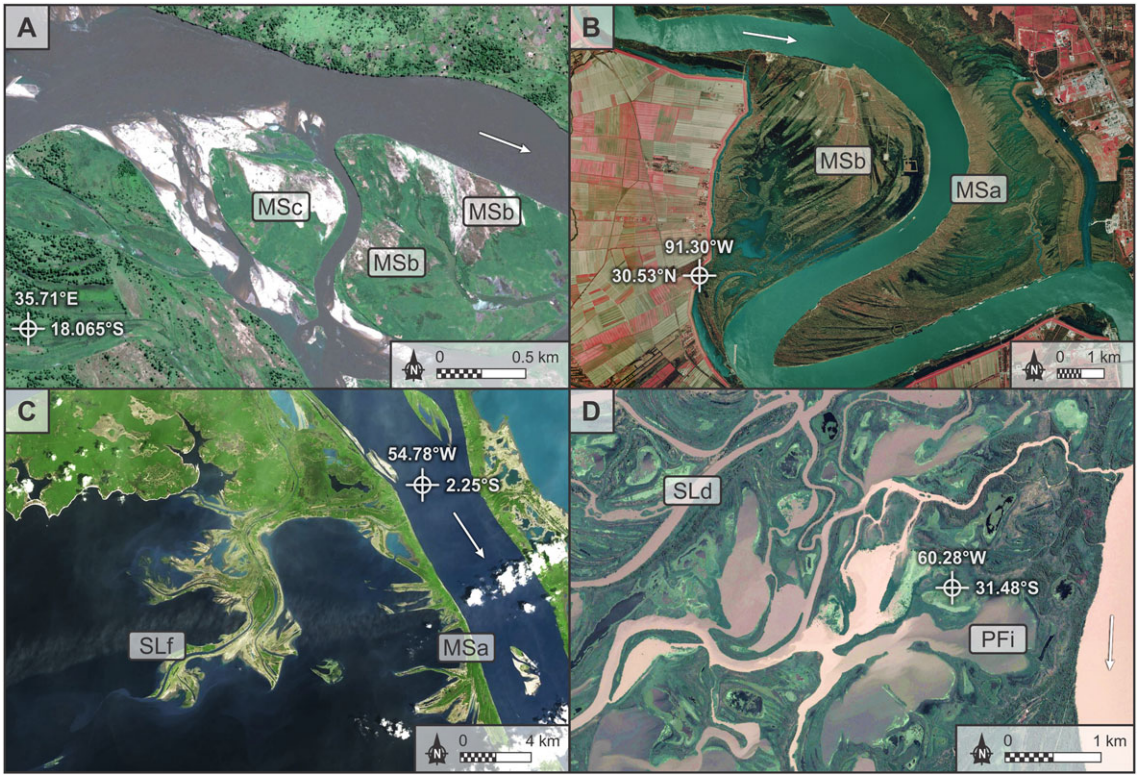

Figure 3. Spillage sedimentation forms on (A) Zambezi River (Map data: Google, DigitalGlobe, April 21, 2013); (B) Mississippi River (Louisiana Oil Spill Coordinator's Office (LOSCO), December 11, 1998, Colour Infrared Orthophoto, NW quadrant of Baton Rouge West Quadrangle, LA, 50:1 MrSID compressed, LOSCO (1998) [c3009139_nws_50]); (C) Amazon (Map data: Landsat - US Geological Survey, October 27, 2013); (D) Rio Paraná (Map data: Google, DigitalGlobe, April 15, 2013). Labels on the figures refer to spillage types identified in Figure 2 and listed in Table I. Satellite data available from the US Geological Survey.

or thousands of years such that breach flows and minor channels are now artificially constrained in some form (Zhuang and Kidder, 2014). Elimination both of palaeochannel and active anabranches as detrimental to agricultural potential or river navigation, bank-breach sealing and bank stabilization (Hohensinner *et al.,* 2014; Klasz *et al.*, 2014; Džubáková *et al.,* 2015), and new floodplain drainage works – all can create new styles of spillage sedimentation in constrained rivers. Levee growth may be increased with catchment settlement and soil erosion (Funabiki *et al.*, 2012). By contrast, large dams, with discharge regulation and sediment storage, have decreased the supply of water and sediment to larger rivers downstream (Syvitski and Kettner, 2011), and thus the potential for sediment spillage. Lateral channel constraint on the formerly multi-channel Danube has led to the 'natural' pioneer growth of a levee over some 100 years in the absence of channel movement (Klasz *et al.*, 2014). A 'great acceleration' of urban and industrial development since c.1945 has led to the increased riverine export of pollutants globally. The quality of spillage sediments on many large rivers has been altered for some centuries as well as their quantity (Middelkoop, 2000). Millennia of accelerating transformation has affected most long-used floodplains such as the Indus (Syvitski and Brackenridge, 2013) or the Hwang He (Yellow River) where Zhuang and Kidder (2014) observe that transformations date from at least the third millennium BCE. Other rivers like the Amazon are, at least as yet, less greatly modified.

Spillage along the Amazon floodplain

Although there have been several recent studies describing the geomorphology and relief of the Amazon River floodplain (Latrubesse and Franzinelli, 2002; Rozo *et al.* 2012; Trigg *et al.*, 2012; Lewin and Ashworth, 2014b) no study has yet systematically identified, interpreted and quantified the type and prevalence of spillage sedimentation that contributes to floodplain development and aggradation. Nor has there yet been a survey of the constituents of a large river floodplain over 100 s of km and down a long profile. Unlike many other large rivers, the Amazon presents the opportunity to quantify floodplain morphology and spillage prevalence for a catchment almost untouched, for now, by major dam construction.

Characteristics of the Amazon Basin

The Amazon River has the largest drainage basin in the world of 6×10^6 km^2 (Figure 5(A)) that covers about 5% of the land on Earth (Filizola and Guyot, 2004). The Amazon is more than 3000 km long, with a mean annual discharge of nearly 210×10^3 m^3 s^{-1} (Park and Latrubesse, 2015), and has three of the world's largest tributaries – the Madeira, Negro, and Japurá (Figure 5(B)). The centre of the Amazon Basin is dominated by Tertiary and Quaternary lacustrine and alluvial deposits of sand and silts, at times weathered to clays, and dissected into a landscape of short 0.05–0.5 km hillslopes (Mertes and Dunne, 2007). The active Holocene floodplain (Figure 5(B)) is inset into Upper Cretaceous, Neogene and Pleistocene terraces. The Holocene Amazon floodplain contains complex anabranching channels with meandering sections of various scales with extensive scroll bars and levees, lakes in channel cutoffs, backswamps, and various other forms of negative relief (Lewin and Ashworth, 2014a, see Figure 1). Large tributary lakes, such as Lago Aruã at the mouth of the Rio Urucu and as at the mouth of the Rio Tapajós, are dammed by the alluvium from the main channel (Ashworth and Lewin, 2012; see Figure 6(B) later). The gradient of the Amazon River varies from

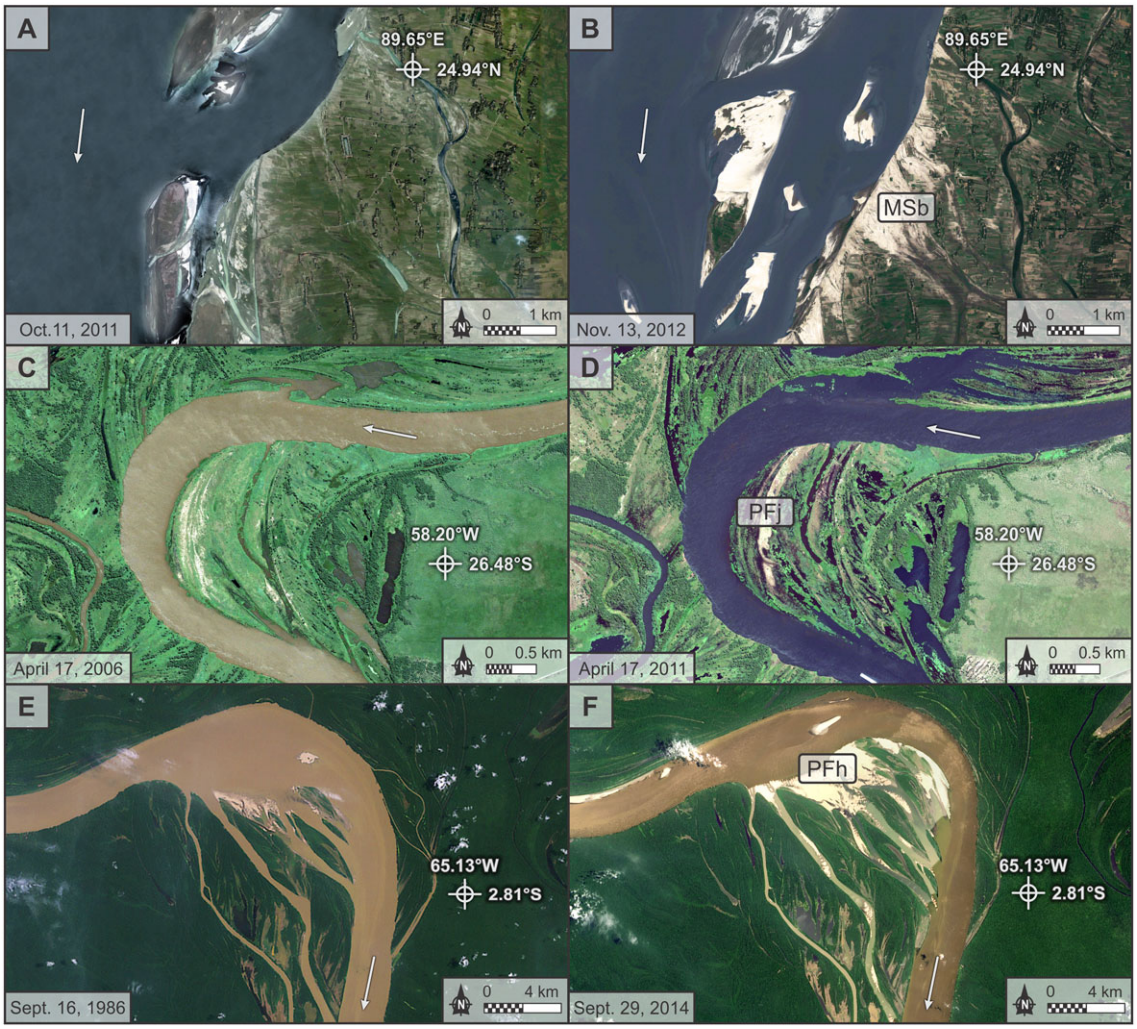

Figure 4. Examples of the variety in timescales for the creation of spillage sedimentation. (A–B) Brahmaputra River before and after a single monsoon season in 2012 (Map data: Google, Digital Globe, October 11, 2011 (A), November 13, 2012 (B)); (C–D) the Rio Paraná over a five year period (Map data: Google, Digital Globe, April 17, 2006 (C), April 7, 2011 (D)); (E–F), the upper Amazon in 1986 and 2014 (Map data: Landsat - US Geological Survey, September 16, 1986 (E) and September 29, 2014 (F)). Labels on the figures refer to spillage types identified in Figure 2 and listed in Table I.

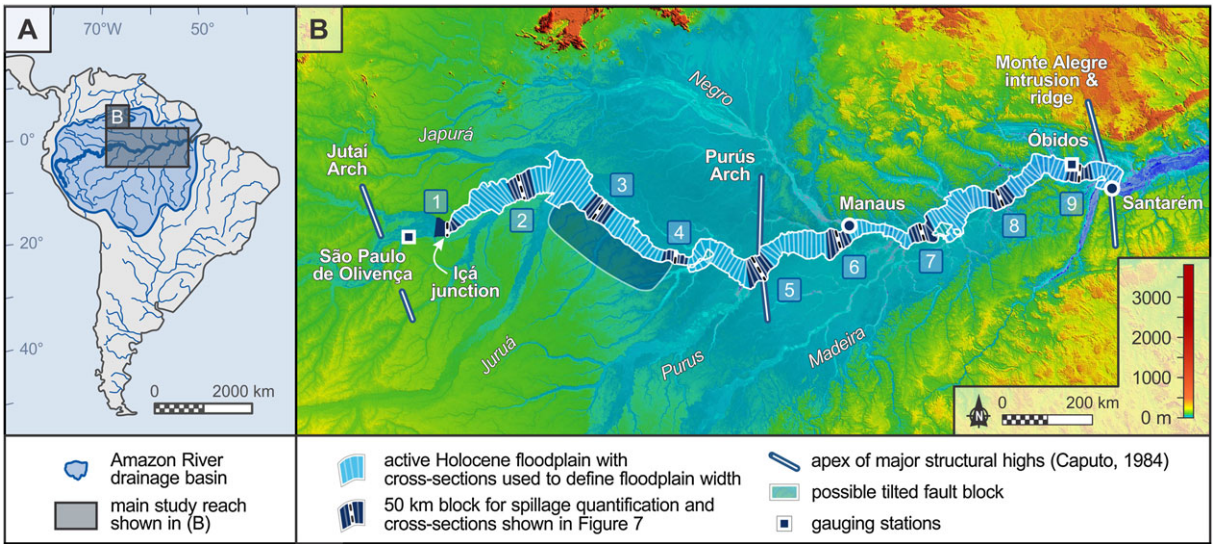

Figure 5. (A) Location map of the Amazon catchment; (B) study reach for floodplain spillage quantification.

0.000040 to 0.000017 along the 1700 km (Figure 6(A)). Mertes *et al.* (1996) and Dunne *et al.* (1998) suggest the regional structural geology may have an influence on the local channel pattern as the Amazon crosses the downstream end of a possible fault block that tilts the valley floor towards the south-southeast (Tricart, 1977) and as it passes over two major

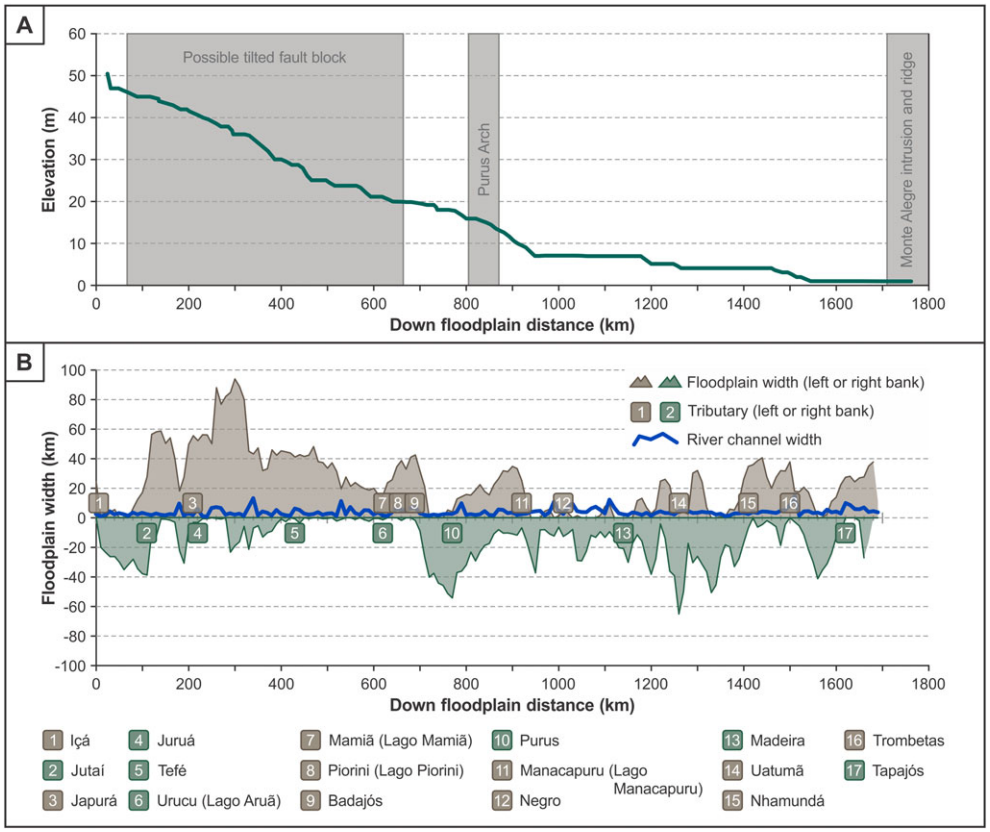

Figure 6. Amazon downstream changes in: (A) water surface slope; (B) left and right bank floodplain width. The long profile was constructed using SRTM data for the water surface elevation, every 10 km, at the centre of the main channel.

structural highs (the Purus Arch and Monte Alegre ridge; see Caputo, 1984). These structural features may cause channel entrenchment and floodplain narrowing, but as Figure 6(B) shows, this is only a weak association and there is no sharp change in either gradient or floodplain width at the interpreted locations of these structural discontinuities.

The Amazon has one of the world's largest sediment loads that can range from 616 Mt. $yr.^{-1}$ at São Paulo de Olivença to 1240 Mt. $yr.^{-1}$ at Óbidos (Dunne *et al.*, 1998, locations in Figure 5(B)). Individual tributaries are important sources of suspended sediment with some tributaries that drain cratons contributing low sediment loads ranging from 10 to 20 Mt. $yr.^{-1}$ (e.g. Negro, Tapajós and Xingu), whereas others such as the Madeira River, that drain the Bolivian and Peruvian Andes, deliver up to 600 Mt. $yr.^{-1}$ (Latrubesse *et al.*, 2005; Park and Latrubesse, 2015).

The Amazon has an extraordinary volume and rate of exchange, of both water and sediment, between the main channels and the floodplain, during the passage of the annual flood wave. Up to 30% of the flow of the mainstem river is derived directly from water stored on the floodplain and from flow from local sources passing through the floodplain (Richey *et al.*, 1989). Rates of water exchange on the Amazon can vary from 5500 $m^3 s^{-1}$ during floodplain infilling to −7500 $m^3 s^{-1}$ during drainage (Alsdorf *et al.*, 2010). Up to 77% of the annual total input of water to the 2430 km^2 Lago Grande de Curuai near Óbidos (Figure 5(B)) is provided directly by the Amazon River (Bonnet *et al.*, 2008).

Flow across the Amazon floodplain is spatially complex for any given time and changes significantly during the passage of the flood wave. During mid-rising water, inundation appears first as a patchwork steered by the floodplain topography of scroll bars, levees, various types of floodplain channels, and depressions, whereas at peak stage, floodplain flow more closely parallels the Amazon River (Alsdorf *et al.*, 2007; see Figure 1). Sediment concentrations from the river are usually higher during rising water (Dunne *et al.*, 1998) and flow patterns at mid-rising times govern deposition (Alsdorf *et al.* 2007). At peak flows the main river may be high in sediment loadings but the potential for spillage is supressed because there is an intangible water barrier at down-river sites where floodplain water levels are already high (Park and Latrubesse, 2015).

Average annual rates of transport over each bank for various reaches of the Amazon during a 16-year period ranged from 30 to 850 t m^{-1} $yr.^{-1}$, depending on the gradient, valley width and sinuosity of each reach (Dunne *et al.*, 1998). Although it has been suggested that downstream delivery of sediments to the Amazon may be modulated by the El Niño/Southern Oscillation (ENSO) cycle, with warm (El Niño) phases causing smaller shorter floods and low sedimentation rates and cold (La Niña) phases causing larger longer floods and high sedimentation rates (Aalto *et al.*, 2003), Lombardo (2016) has shown that in the headwaters of the Amazon there is no correlation between the frequency of crevasse splays and ENSO events, and intrabasinal processes on a year to decade timescale are more important controls on sediment delivery and crevasse spillage sedimentation.

Study area and analysis

A 1700 km reach of the Solimões-Amazon River and floodplain (it becomes the Amazon after the confluence with the Negro River, see Figure 5(B)) was selected from where the Rio Içá joins the Solimões River at Santo Antônio do Içá to where the Rio Tapajós joins the river at Santarém (Figure 5(B)). This study reach was selected so that it captured most of the major tributaries of the Amazon and avoided significant backwater effects from marine tides. At Santarém, which is 775 km from the Amazon

mouth, the semi-diurnal tidal wave amplitude is a maximum of 0.2 m at river low flow in November and negligible at river high flow in June (Kosuth *et al.,* 2009).

A mosaic of Digital Elevation Models (DEMs) was built based on the US Geological Survey (USGS) SRTM dataset at 1 arc second (30 m) resolution. The vertical resolution of the SRTM data is +/− 10 m. Satellite images from the USGS Landsat 8 program were also downloaded and cropped to the study area to aid in characterization of spillage phenomena. Satellite images were sourced from low flow months to facilitate visibility of floodplain spillage forms. The margins of the Holocene floodplain were defined by constructing cross-sections at 10 km intervals (see locations in Figure 5(B)) and highlighting step-changes in floodplain elevation (typically 20–30 m).

The study area was divided into nine floodplain 'blocks' (Figure 5(B)), spaced at 200 km intervals downstream. Each floodplain block is 50 km long (25 km either side of the 200 km spacing points) and included both a SRTM DEM and a Landsat 8 satellite image. Each block was loaded into Global Mapper™ and polygon features were drawn manually around each spillage feature using the classification scheme in Table I, together with associated water elements (e.g. main river channel, accessory channels, floodplain water bodies).

Spillage sedimentation along the Amazon floodplain

Figure 6(B) shows the changes in floodplain width downstream and therefore the potential floodplain space for spillage sedimentation. Neither the Amazon main channel nor its floodplain simply increases in width downstream as major tributaries contribute their discharges (for the Amazon network, see Weissmann *et al.*, 2015, their Figure 23). The maximum floodplain width is ~110 km at 300 km downstream where the Japurá tributary/fan merges with the Solimões floodplain. The joining of each tributary causes an immediate increase in floodplain width – though to some extent this is also a consequence of the amalgamation of two independent floodplains (Figure 6(B)). The Amazon appears to oscillate within its Holocene floodplain with a preference for the floodplain to be on the left bank in the upstream portion of the study reach and on the right once the Purus tributary enters at ~750 km (Figure 6 (B)). A similar observation of large-scale channel belt oscillation was made for the Brahmaputra by Thorne *et al.* (1993) where it was suggested that the wavelength of the sinuous braid-belt scaled with the valley width rather than that of the main channel.

Figure 7 shows the relief on the floodplain that is typically 5–20 m in between expansive (up to 10 km wide) lakes and channels. SRTM data is accurate only to +/− 10 m in the vertical and cannot distinguish between a vegetation canopy and bare floodplain surface. But the floodplain relief is remarkably consistent along each cross-section and in most cases it is relatively easy to define active floodplain width on a morphological basis (see Figure 7, shaded area).

Figure 8 shows the interpretation of three 50 km floodplain blocks at 0 km, 800 km and 1600 km downstream of the Rio Içá. Only six spillage form types as listed in Table I were identified in the imagery partly because individual elements were too small to identify and then represent as polygons. Diffuse overbank spreads (PFk) also cannot be readily distinguished from imagery. Spillage types PFh and PFj that are associated with meander bend evolution and scroll bar growth are here amalgamated into one group called 'point bar complexes' (PBC). If there were no spillage sedimentation forms, or no unambiguous evidence for spillage, the floodplain was classified as UF or 'undifferentiated floodplain'. Inevitably, some of the UF will be older fragments of floodplain relief and spillage sedimentation that has been covered by organic-rich fine material and subsequently masked by vegetation.

The frequency of occurrence of different spillage types on the Amazon floodplain over the 1700 km study reach is summarized in Table 2 and Figure 9(A), (B). There is no consistent trend in the change in MSa, MSb, MSc or SLd downstream and neither of these spillage form elements constitutes more than 5% of the floodplain, though levee sedimentation (MSa)

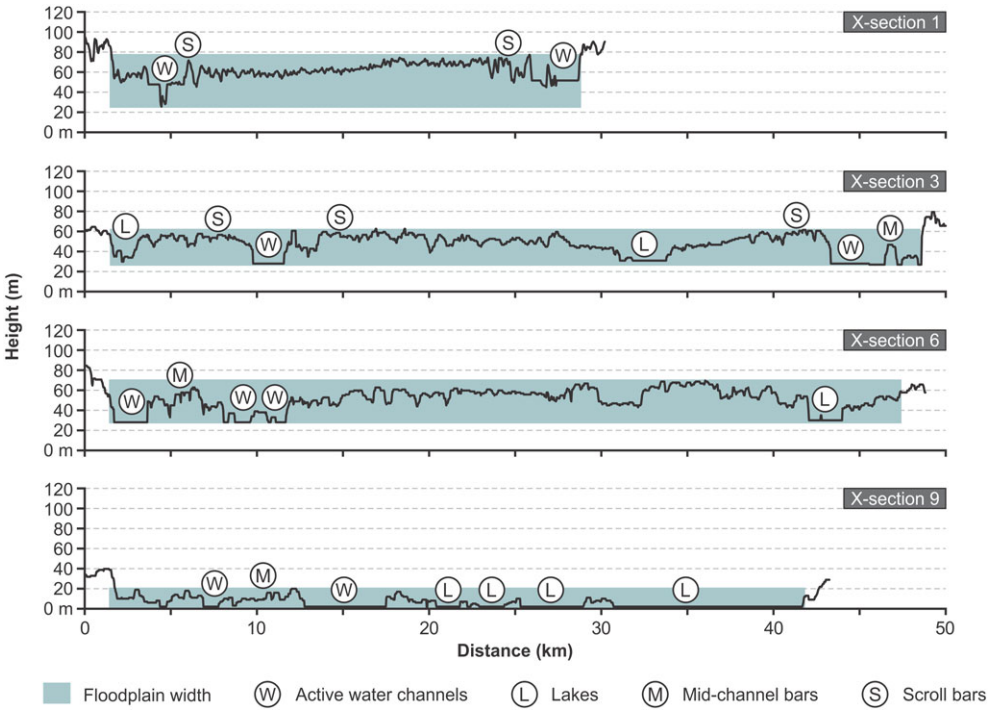

Figure 7. Representative cross-sections of the Amazon floodplain abstracted from SRTM data (acquired on February 11–22, 2000). Profile locations are shown in Figure 5B. SRTM data available from the US Geological Survey.

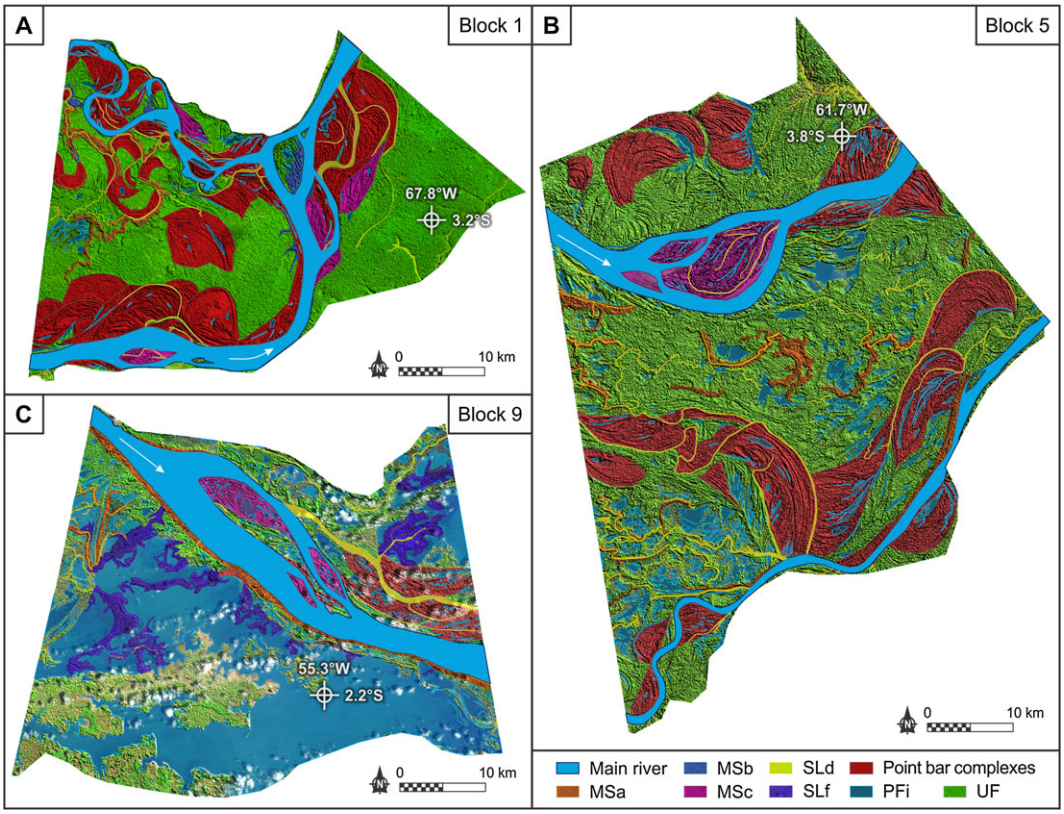

Figure 8. Three of the 50 km long floodplain blocks used to quantify the prevalence of different spillage sedimentation on the Amazon. Block locations are shown in Figure 5(B). The interpreted spillage forms are shown superimposed on the original SRTM image. SRTM image acquisition spans February 11, 2000 to February 22, 2000 but all were taken at low flow. Satellite data available from the US Geological Survey.

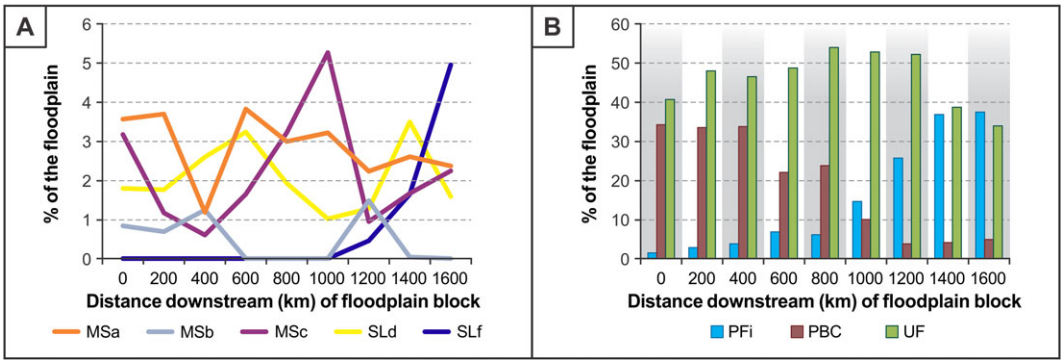

Figure 9. Amazon downstream changes in (A) Percentage of floodplain occupied by MSa-MSc and SLd-SLf (see Table I) spillage elements; (B) percentage of floodplain occupied by waterbodies (PFi), point bar complexes (PBC) and undifferentiated floodplain (UF) (where there is no clear evidence of spillage forms). Note the floodplain extent on block 6 (centred on 1000 m downstream) is not based on an abrupt elevation change at the margins or mapping of alluvial morphologies and instead is adjusted to match the floodwater limits as mapped by Hess *et al.* (2003) which reduces the total floodplain area.

is prevalent in all floodplain blocks. Bank top splays (MSb) are mostly absent for much of the river, but in particular in the downstream reaches, which is expected given bank top splays are likely to be made up of mostly coarser sediment.

As Figure 8(A) shows, the upper reaches of the Amazon floodplain are dominated by recent and Holocene scroll bar formation (PBC) but this mode of sedimentation and potential for spillage decreases consistently downstream so that only 4% of the floodplain is scroll bars at 1600 km (Table II, Figure 9). The downstream decrease in frequency of PBC in the floodplain correlates with a reduction in percentage area of total channel change ($r^2 = 0.60$) as measured by Mertes *et al.* (1996, their Figure 8, p. 1097) that is attributed to the transition from actively migrating sinuous main and floodplain channels to a more confined and straight channel system.

There is a steady increase in the presence of water bodies and therefore the potential for ponded lake sedimentation (PFi) from up to downstream (Table II, Figure 9(A), (B)). Note, water bodies are taken as an indicator of potential PFi, though the former is a topographic feature, while the latter describes the process of infilling/spillage. The downstream increase in the presence of water bodies is the inverse of the situation for PBC described above. This probably reflects the progressive downstream change from a laterally mobile channel and reworked floodplain to spillage into water-filled voids left by a relatively immobile main channel and topography developed during the time of lower Holocene sea level. Water body area increases exponentially downstream ($r^2 = 0.93$) and Mertes *et al.*, (1996) note that the water bodies also become rounder downstream. With an increase in PFi downstream, there is a

Table II. Percentage area of different spillage forms for nine 50 km blocks of the Amazon floodplain over a downstream distance of 1700 km

		Percentage of floodplain								
Block	Distance downstream (km)	MR	MSa	MSb	MSc	SLd	SLf	PFi	PBC	UF
1	0	14.3	3.6	0.8	3.2	1.8	0	1.5	34.2	40.7
2	200	8.4	3.7	0.7	1.2	1.8	0	2.8	33.5	48
3	400	10.4	1.2	1.2	0.6	2.6	0	3.8	33.7	46.5
4	600	13.7	3.8	0	1.6	3.2	0	6.8	22	48.7
5	800	8.1	3	0	3.2	1.9	0	6.1	23.8	53.9
6	1000	13.1	3.2	0	5.3	1	0	14.6	10	52.8
7	1200	12	2.2	1.5	0.9	1.3	0.5	25.7	3.8	52.2
8	1400	11	2.6	0	1.7	3.5	1.6	36.8	4.1	38.7
9	1600	12.6	2.4	0	2.2	1.6	5	37.4	4.9	33.9

MR = Main River, MSa = Levees; MSb = Bank-top splays; MSc = Channel bars and islands; SLd = Accessory channels; SLf = Crevasse with deltas; PFi = Ponded lakes and water bodies, PBC = Point Bar Complexes, and UF = Undifferentiated Floodplain. Locations of the blocks are shown in Figure 5(b). Note the floodplain extent on block 6 is not based on an abrupt elevation change at the margins or mapping of alluvial morphologies and instead is adjusted to match the floodwater limits as mapped by Hess et al. (2003) which reduces the total floodplain area.

corresponding increase in the presence of inland delta formation (SLf). Around 40% of the Amazon floodplain either shows no discrete spillage forms, is masked by forest, or forms are too small/local to allow quantification from the imagery.

Diversity and presence of spillage forms on large rivers

To compare the range of spillage possibilities globally, Table III lists reaches on 20 of the world's largest rivers, together with their spillage forms and showing also ones that dominate. Reaches are again of approximately 50 km in length. Spillage form presences are diverse, as are floodwater dispersion routes via channeled and unchanneled flows (cf. Rudorff *et al.*, 2014). Two sites are given for the Amazon to emphasize the down-valley change previously discussed; large rivers seldom maintain form constancy or sedimentation patterns throughout even their lower reaches.

Main channel margins

Only a few large rivers without rapid lateral migration have prominent levees (MSa), notably the lower Mekong where the lengthy mountain course exits to cross a broad depression. Other rivers may have sets of smaller levees stacked laterally where rivers oscillate from side to side (middle Amazon; Latrubesse and Franzinelli, 2002). The presence on the Mississippi of both levee and migration swales is unusual and perhaps surprising. Levees depend on the short-distance dispersion of bed materials as well as finer suspended sediment diffusion. Bed material splays (MSb) along braided channels may form diffuse patches along 100 s of metres of channel bank (Jamuna, Figure 4(B)). Splay material may also be fed through crevasses or along palaeochannel depressions to much greater distances laterally. In anabranching systems, sedimentation capping bars and islands (MSc) is very common.

Secondary linear systems

Channelized dispersion (SLd) is important on multi-channel reaches with prominent secondary channels (Orinoco, Yenisei, Volga, Lena, Paraná). Secondary branches with limited lateral mobility disperse a generally finer fraction of mainstream sediment loadings considerable distances across basins and container valleys. Others have multiple meandering channels (Ob, Volga) each of which has been laterally active.

Crevasses (SLe) may be cut through previously formed levees (Figure 3(C)). Splays are particularly prominent on the Mekong, as previously noted, with high (also breached) levees. Upstream of the delta, many smaller ones are artificial, spreading cultivable material at flood stage without overtopping levees and their strings of settlement. As previously demonstrated, crevasse breaches leading to lake delta sedimentation (SLf) are a feature of the lower Amazon.

Linear dispersion can also relate to presently or formerly active avulsing main channels. Chen *et al.* (2012) and Syvitski and Brackenridge (2013) have emphasized the extreme importance of avulsion processes along the Yellow and Indus rivers. Over a longer timespan, Morozova (2005) pointed to the possible role of avulsion in affecting the fortunes of Mesopotamian cultures, while the Holocene Mississippi was characterized by avulsive relocation of its meander belts (Saucier, 1994).

Prior-form following

Linear and localized infills in swales and palaeochannels (PFh, PFj) are common on more than half of the reaches examined (Table III); these are on middle reaches at steeper gradients reflecting previous lateral channel migration.

The contrasting feature alongside distal reaches of many large rivers (Amazon, Magdalena, Mississippi, Paraná, Yangtze) is that they have quasi-permanent floodplain water bodies (Paira and Drago, 2007; Ashworth and Lewin, 2012) and sedimentation here may be in the form of diffuse lentic (still water) sedimentation (PFh), floodplain deltas (SLf) and channels developed by subaqueous levee extension (Figure 3(C)).

It is also striking that, even where channel banks are not continuous (e.g. the Lago Cabaliana at Manacapuru on the Amazon, 3° 17′S, 60° 38′W), there exists a hydraulic barrier to sediment spillage. This is because water elevations on the floodplain are already high; sedimentation thus depends very much on existing floodplain water levels at the time of mainstream high sediment loadings. Conditions may be such that, largely free of mineral contamination, extensive *in situ* organic sedimentation can be generated in floodplain waterbodies or wetlands.

Changing river stage

The important role of stage levels may be illustrated by spillage on the lower Amazon (Figure 10). Park and Latrubesse (2015)

Table III. Prevalence of spillage sediment forms on large river floodplains

River	Lat (°)	Long (°)	Floodplain width (km)	CP	MSa	MSb	MSc	SLd	SLe	SLf	SLg	PFh	PFi	PFj	PFk	Dominating features
Amazon*	2°33′ S	66°30′ W	40	m/i	—	—	●	●	◦	—	◦	●	◦	◦	—	Inter-bar, chute and older palaeochannel fills
Amazon†	2°00′ S	55°32′ W	40	m/i	●	—	◦	◦	◦	●	◦	—	●	—	◦	Lake deltas and subaqueous levees
Congo	2°09′ N	21°36′ E	8	s/i	—	—	●	◦	—	—	◦	—	—	—	—	Island generation
Orinoco	7°44′ N	65°50′ W	18	b	—	—	●	●	—	—	◦	●	◦	●	—	Multiple channels with fills
Yangtze	30°37′ N	117°13′ E	23	m/i	●	—	●	—	—	◦	◦	◦	◦	◦	◦	Levees, basins and lakes
Brahmaputra	25°50′ N	89°50′ E	22	b	—	◦	●	◦	—	—	—	●	—	—	—	Migrating braid belt with banktop splays, some into palaeochannels
Yenisei	65°16′ N	87°56′ E	9	s	—	—	—	●	—	—	◦	◦	●	●	—	Islands, swales, multiple thaw lakes
Volga	47°07′ N	47°18′ E	14	a/i	—	◦	●	●	—	—	◦	●	◦	●	—	Linear fills and lakes; some splays
Zambezi	17°57′ S	35°30′ E	9	m/i	—	◦	●	◦	—	—	◦	●	◦	●	—	Linear fills and lakes; some splays
Lena	62°42′ N	129°49′ E	8	b/m/i	—	◦	●	●	—	—	◦	●	●	●	—	Braid bar islands, secondary channels
Mississippi	30°45′ N	90°33′ W	34	m	●	◦	—	—	—	—	—	●	—	◦	◦	Levees, palaeochannel and swale fills
Mekong	12°15′ N	105°42′ E	10	s/i	●	—	◦	◦	●	◦	◦	—	—	—	◦	Island generation, levees, basins, splays and secondary channels
Paraná	31°34′ S	60°26′ W	33	m/i	—	—	●	●	—	—	◦	●	●	◦	◦	Lakes with secondary channel ridges and swale fills
Ob	58°20′ N	82°40′ E	23	m/i	—	—	●	◦	—	—	◦	●	●	●	—	Meander plain with palaeochannel fills and secondary channels
Ganges	25°24′ N	83°10′ E	6	m/i	—	—	◦	◦	—	—	—	—	—	—	●	Diffuse sedimentation
Amur	48°48′ N	135°46′ E	10	s/m/i	—	—	●	◦	—	—	◦	●	●	●	—	Multiple channels with palaeochannel and swale fills
Mackenzie	64°38′ N	125°03′ W	6	i	—	—	●	◦	—	—	◦	—	◦	◦	—	Multiple channel fills
Columbia	45°46′ N	120°48′ W	8	s	—	—	—	◦	—	◦	◦	●	◦	◦	—	Palaeochannel and swale fills
Indus	27°20′ N	68°15′ E	77	b	—	◦	●	◦	—	—	—	●	—	●	◦	Active and inactive braidplain
Magdalena	9°08′ N	74°44′ W	43	a	●	—	—	◦	◦	◦	—	◦	●	—	—	Subaqueous and exposed levees, splays, and deltas
Danube	46°14′ N	18°53′ E	16	m	—	—	—	—	—	—	—	●	—	●	◦	Meander plain with palaeochannel fills

CP = Channel pattern: (b) braided, (m) meandering, (s) straight, (a) anastomosing, (i) anabranching, with islands. MSa = Levees; MSb = Bank-top splays; MSc = Channel bars and islands; SLd = Accessory channels; SLe = Crevasse splays; SLf = Crevasse with deltas; SLg = Internal drainage nets; PFh = Cutoff and palaeochannel fills; PFi = Ponded lake filling; PFj = Point bar swales and chutes; PFk = Diffuse overbank spreads. (● prominent, ◦ present, — not extensive)

*Amazon reach 1

†Amazon reach 2

Figure 10. Response of spillage activity to a change in stage on the Amazon. Label on Figure 10(B) refers to the spillage type identified in Figure 2 and listed in Table I. Label Z on Figure 10(B) is discussed in the text. Satellite data available from the US Geological Survey.

show peak river sediment concentrations in October–January ahead of peak water discharges in May–June; lake sediment accumulation occurs during this flood rise (Maurice- Bourgoin *et al.*, 2007). Figure 10(A) shows a single crevasse through a levee with a sediment plume entering the sediment-free Rio Negro that joins the Amazon some 10 km further downstream. At a higher stage (Figure 10(B)), multiple trans-levee overflows are operating with the diffuse spread of sediment. Lake and tributary levels relative to river levels are crucial in the spillage process. Park and Latrubesse (2015) showed (their Figure 7) the varying relationship between inundation extent and the sediment concentration in inundated areas, with low concentrations at peak flow in May–August, while Maurice-Bourgoin *et al.* (2005, 2007) demonstrated the complex nature of the balance between input, accumulation and also channel-return for lake sediment. The areas actually flooded on large rivers, and the cumulative process of spillage sedimentation, is often intricate and complex (Gan *et al.,* 2012).

Dryland rivers

Dryland rivers may exhibit different spillage forms because they often experience downstream diminution of flows such that spillage is represented by floodout splays as water is lost (Tooth, 1999, 2005). Some 60% of the Earth surface's modern basin area has an arid climate (Nyberg and Howell, 2015) and 18% of continental land has endorheic drainage, both to small intermontane basins and to very large ones such as Lake Eyre in Australia (1 200 000 km^2), the Aral (1 549 000 km^2) and Caspian (3 626 000 km^2) Seas in Asia, and Lake Chad in Africa (2 434 000 km^2). Present day individual and ephemeral rivers are not generally in the 'large' category, but earlier Holocene conditions with greater runoff produced greatly expanded lakes and some large overflow rivers like the drainage of Chad through to the Atlantic via the Benue. Indeed recent work by Skonieczny *et al.* (2015) suggests that 'African Humid Periods' from at least 245 ka, and most recently 11.7–5.0 ka, triggered the reactivation of an ancient river system, the Tamanrasett, which may have ranked as the 12th largest drainage basin worldwide – yet today no major river exists in the area.

Some large rivers lose most of their flow, and sediment, in dryland basins along their courses, as in the Inner Niger Delta in Mali (Figure 11(A), (B)). Here a distributary channel system operates during the wet season despite water loss at the margins of the channel network (Figure 11(C)). Sediment spillage takes the form of low relief (typically <4 m) levees (MSa) that border individual distributaries, or a mosaic of bank-top splays (MSb) that are formed by overbank sedimentation from distributary channels that migrate back-and-forth across a series of narrow (<600 m) active deposition zones. In the dry season (Figure 11(D)) the spillage forms are exposed as a series of sinuous 'tentacles' of sedimentation (see also Tooth and McCarthy, 2007).

Global climate contrasts

Table IV advances a rationalization for the distribution of the spillage sedimentation forms, in particular based on prior floodplain water status as highlighted in the previous sections. Altogether, style dominance depends on three main factors: (a) diverse sediment loadings and floodwater discharges; (b) the floodplain topography present (including both channel bank/alluvial ridge levels in relation to their floodplains, channeling palaeoforms, and developed connectivities between negative floodplain relief elements); and (c) prior inundation status, in the form of lakes and their levels, wetlands, or (initially) dry land. This third factor relates to *local* precipitation inputs and floodplain water levels that mainstream flows and transported sediments are spilling across. It is suggested that local climates, as well as large river inputs and floodplain morphology, are reflected in the styles of spillage sedimentation.

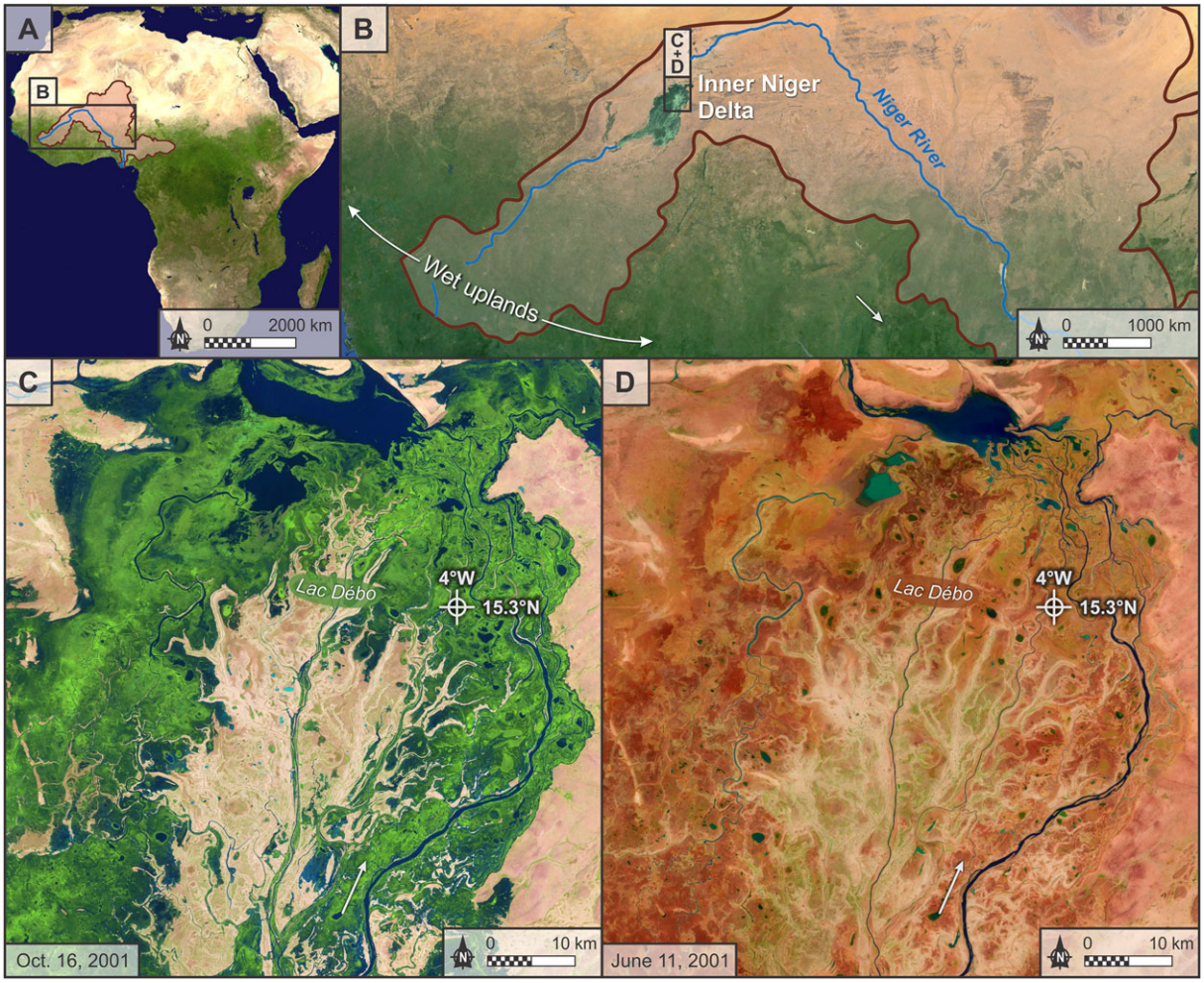

Figure 11. Dryland river spillage on the Inner Niger River (Macina), Central Mali, C: wet season; D: dry season. Note the tentacles of spillage forms along distributary channels but the general absence of 'terminal splays'. Several isolated waterbodies become connected during the wet season and vegetation growth (green colour in C) is abundant. C and D courtesy of MDA Federal (2004), Landsat GeoCover ETM+ 2000 Edition Mosaics, USGS, Sioux Falls, South Dakota, 2000. C and D satellite data available from the US Geological Survey with C taken on 16 October 2001 and D on 11 June 2001.

Table IV. Spillage styles in different environments

	Wetland	Intermediate	Dryland
Diffuse	Lacustrine fills	Levees, banktop splays, overbank sedimentation	Levees
Linear (palaeoform-following)	Main channel slackwater and backwater fills	Palaeochannel and swale fills	Palaeoform-following
Linear (auto-generated)	Subaqueous levees	Crevasse splays and network extension	Floodout splays

Conclusions

Out-of-channel sedimentation and dispersion along the world's largest rivers are both complex and geographically variable. Using remote sensing imagery and from detailed mapping of floodplain sedimentation types it has been shown that out-of-channel sedimentation processes alongside large rivers can be divided into 11 styles and characterized collectively as 'spillage phenomena'. Many are not strictly 'overbank' in nature, but rather penetrate floodplains via accessory or tributary channels, or through depressions in bank elevation determined by prior channel activity. Three logical groupings of these spillage sedimentation styles have been distinguished – 'mainstream sediments', 'secondary linear systems' and 'prior-form filling'.

Systematic mapping of spillage forms along 1700 km of the Solimões-Amazon shows there are quantitative down-valley trends. Accretion swale and lacustrine fills dominate in different parts; other mainstream features (like levees) have limited prevalence and spatial coverage, while strings of sediment from accessory channels are common, in some places prograding across and bridging lakes, and elsewhere developing their own morphologies by lateral erosion and sedimentation.

Globally there is considerable spillage variety such that the Amazon should not be taken as 'typical'. In addition to simple planar spread, the active 'overbank domain' in different large river reaches may or may not include: island build-up; levees; bank top splays; crevasse channels extending to splay fans; accessory channel sedimentation; deltas and linear channels prograding across wetlands and ponded lakes; scour through internal drainage connections and network extension created following flood flows; lateral accretion infills; and lacustrine sedimentation.

Spillage sedimentation diversity on large river floodplains has been under-represented in alluvial depositional models. In certain places, the totality of these processes currently contributes more to fills now being preserved than channel accretion. Lower reach main rivers that show limited lateral activity within container valleys or basins leave spillage to dominate floodplain sedimentation processes.

A caveat is that many large rivers have been transformed by anthropogenic activity, so that discharges and sediment loadings, and therefore spillages, are effected by upstream factors such as soil erosion, pollutant inputs and river regulation. However, finer sediments are still widely subjected to flood stage spillage and dispersion. Global surveys of spillage opportunity and type prevalence could help identify, track and mitigate the risk of potential pollution incidents and catastrophic infrastructure failure such as mine tailings dam failures.

Acknowledgements—PJA thanks the UK Natural Environment Research Council (NERC) for a collaborative grant NE/E016022/1 on large rivers that prompted some of the ideas reported here. RS is grateful to the NERC for a PhD studentship NE/K501281/1 that generated some of the Amazon data reported here. Chris Simpson kindly produced the figures. We are pleased to acknowledge the helpful review comments from Tom Dunne and an anonymous referee.

References

Aalto R, Maurice-Bourgoin L, Dunne T, Montgomery DR, Nittrouer CA, Guyot JL. 2003. Episodic sediment accumulation on Amazonian floodplains influenced by El Nĩno/Southern Oscillation. *Nature* **425**: 493–497. DOI:10.1038/nature02002.

Aalto R, Lauer JW, Dietrich WE. 2008. Spatial and temporal dynamics of sediment accumulation and exchange along Strickland River floodplains (Papua New Guinea) over decadal-to-century timescales. *Journal of Geophysical Research* **113** . DOI:10.1029/2006JF000627. F01S04

Adams PN, Slingerland RL, Smith ND. 2004. Variations in natural levee morphology in anastomosed channel floodplain complexes. *Geomorphology* **61**: 127–142. DOI:10.1016/j.geomorph.2003.10.005.

Alexander J, Fielding CR, Pocock GD. 1999. Flood deposits of the Burdekin River, tropical north Queensland, Australia. In Floodplains: Interdisciplinary Approaches, Marriott SG, Alexander J (eds), Vol. **163**. Geological Society London Special Publication: London; 27–40.

Allison MA, Kuehl SA, Martin TC, Hassan A. 1998. The importance of floodplain sedimentation for river sediment budgets and terrigenous inputs to the ocean: insights from the Brahmaputra-Jamuna rivers. *Geology GSA* **26**: 175–178.

Alsdorf D, Bates P, Melack J, Wilson M, Dunne T. 2007. The spatial and temporal complexity of the Amazon flood measured from space. *Geophysical Research Letters* **34** . DOI:10.1029/2007GL029447. L08402

Alsdorf D, Han S-C, Bates P, Melack J. 2010. Seasonal water storage on the Amazon floodplain measured from satellites. *Remote Sensing of Environment* **114**: 2448–2456. DOI:10.1016/j.rse.2010.05.020.

Ashworth PJ, Lewin J. 2012. How do big rivers come to be different? *Earth-Science Reviews* **114**: 84–107. DOI:10.1016/j.earscirev.2012.05.003.

Assine ML, Soares P. 2004. Quaternary of the Pantanal, west-central Brazil. *Quaternary International* **114**(1): 23–34.

Assine ML, Corradini FA, de Pupim FN, McGlue MM. 2014. Channel arrangements and depositional style in the São Lourenço megafan, Brazilian Pantanal wetland. *Sedimentary Geology* **301**: 172–184. DOI:10.1016/j.sedgeo2013.11.0007.

Aufdenkamp AL, Mayorga E, Raymond PA, Melack JM, Doney SC, Alin SR, Aalto RE, Yoo K. 2011. Riverine coupling of biogeochemical cycles between land, oceans and atmosphere. *Ecology and Environment* **9**: 53–60. DOI:10.1890/100014.

Bätz N, Verrreccia EP, Lane SN. 2015. Organic matter processing and soil evolution in a braided river system. *Catena* **126**: 86–97.

Benedetti MM. 2003. Controls on overbank deposition in the Upper Mississippi River. *Geomorphology* **56**: 271–290. DOI:10.1016/SO169-555X(03)00156-9.

Bogen J. 1982. Morphology and sedimentology of deltas in fjord and fjord valley lakes. *Sedimentary Geology* **36**: 245–267.

Bonnet MP, Barroux G, Martinez JM, Seyler F, Moreira-Turcq P, Cochonneau G, Melack JM, Boaventura G, Maurice-Bourgoin L, Leon HG, Roux E, Calmant S, Kosuth P, Guyot JL, Seyler P. 2008. Floodplain hydrology in an Amazon floodplain lake (Lago grande de Curuaí). *Journal of Hydrology* **349**: 18–30. DOI:10.1016/j.jhydrol.2007.10.055.

Brierley GJ, Ferguson RJ, Woolfe KJ. 1997. What is a fluvial levee? *Sedimentary Geology* **114**: 1–17.

Bristow CS. 1987. Brahmaputra River: channel migration and deposition. In Recent Developments in Fluvial Sedimentology, Ethridge FG, Flores RM, Harvey MD (eds). Special Publication 39, Society Economic Palaeontology and Mineralogy: Tulsa, Oklahoma, USA; 63–74.

Bristow CS, Skelly RL, Ethridge FG. 1999. Crevasse splays from the rapidly aggrading sand-bed, braided Niobara River, Nebraska: effect of base level rise. *Sedimentology* **46**: 1029–1047.

Caputo MV. 1984. Stratigraphy, tectonics, paleoclimatology, and paleogeography of northern basins of Brazil. Unpublished PhD thesis, Santa Barbara, University of California.

Cazanacli D, Smith ND. 1998. A study of morphology and texture of natural levees – Cumberland Marshes, Saskatchewan, Canada. *Geomorphology* **25**: 43–55.

Chen Y, Overeem I, Syvitski JPM, Gao S, Kettner AJ. 2011. Controls of levee breaches on the Lower yellow River during the years 1550–1855. In River, Coastal and Estuarine Morphodynamics RCEM2011. Tsinghua University Press: Beijing; 617–633.

Chen Y, Syvitski JPM, Gao S, Overeem I, Kettner AJ. 2012. Socio-economic impacts on flooding: a 4000-year history of the Yellow River, China. *Ambio* **41**: 682–698. DOI:10.1007/s13280-012-0290-5.

Citterio A, Piégay H. 2009. Overbank sedimentation rates in former channel lakes: characterization and control factors. *Sedimentology* **56**: 461–482.

Coleman JM. 1969. Brahmaputra River: Channel processes and sedimentation. *Sedimentary Geology* **3**: 129–139.

Constantine JA, Dunne T, Piégay H, Kondolf M. 2010. Controls on the alluviation of oxbow lakes along the Sacramento River, California. *Sedimentology* **57**: 389–407.

Constantine JA, Dunne T, Ahmed J, Legleiter C, Lazarus ED. 2014. Sediment supply as a driver of river meandering and floodplain evolution. *Nature Geoscience* **7**: 899–903. DOI:10.1038/NGEO2282.

Day G, Dietrich WE, Rowland JC, Marshall A. 2008. The depositional web on the floodplain of the Fly River, Papua New Guinea. *Journal of Geophysical Research* **113** . DOI:10.1029/2006JF000622.F01S02

Dieras PL, Constantine JA, Hales TC, Piégay H, Riquier J. 2013. The role of oxbow lakes in the off-channnel storage of bed material along the Ain River, France. *Geomorphology*. DOI:10.1016/j.geomorph.2012.12.024.

Drago EC. 2007. The physical dynamics of the river–lake floodplain system. In The Middle Paraná River, Iriondo MH, Paggi JC, Parma MJ (eds). Springer-Verlag: Berlin; 53–81.

Dunne T, Aalto RE. 2013. Large river floodplains. In Treatise on Geomorphology, Shroder JF (ed), Vol. **9**. Academic Press: San Diego, CA; 645–678 .DOI: 10.1016/B978-0-12-374739-6.00258-X

Dunne T, Mertes LAK, Meade RH, Richey J, Forsberg BR. 1998. Exchanges of sediment between the floodplain and channel of the Amazon River in Brazil. *Geological Society of America Bulletin* **110**: 450–467.

Džubáková K, Piégay H, Riquier J, Trizna M. 2015. Multi-scale assessment of overflow-driven lateral connectivity in floodplain and backwater channels using LiDAR imagery. *Hydrological Processes* **29**: 2315–2330. DOI:10.1002/hyp.10361.

Farrell KM. 2001. Geomorphology, facies architecture, and high resolution, non-marine sequence stratigraphy in avulsion deposits, Cumberland Marshes, Saskatchewan. *Sedimentary Geology* **139**: 93–150.

Ferguson RI, Werritty A. 1983. Bar development and channel change in the gravelly River Feshie, Scotland. In Modern and Ancient Fluvial Systems, Collinson JD, Lewin J (eds), Vol. **6**. International Association of Sedimentologists Special Publications: Blackwell, Oxford; 181–193.

Ferguson RJ, Brierley GJ. 1999. Levee morphology and sedimentology along the lower Tuross River, south-eastern Australia. *Sedimentology* **46**: 627–648.

Fielding CR, Ashworth PJ, Best JL, Prokocki EW, Sambrook Smith GH. 2012. Tributary, distributary and other fluvial systems: what really represents the norm in the continental rock record? *Sedimentary Geology* **261–262**: 15–32. DOI:10.1016/j.sedgeo.2012.03.004.

Filizola N, Guyot JL. 2004. The use of Doppler technology for suspended sediment discharge determination in the River Amazon. *Hydrological Sciences Journal* **49**: 143–153.

Fryirs KA, Brierley GJ. 2013. Floodplain forms and processes. In Geomorphic Analysis of River Systems: an Approach to Reading the Landscape, Fryirs KA, Brierley GJ (eds), 1st edn. Blackwell: Chichester, UK; 155–173.

Funabiki A, Saito Y, Phai VV, Hieu N, Haruyama S. 2012. Natural levees and human settlement in the Song Hong (Red River) delta, northern Vietnam. *The Holocene* **22**: 637–648. DOI:10.1177/0959683611430847.

Gan TY, Zunic F, Kuo C-C, Strobl T. 2012. Flood mapping of Danube River at Romania using single and multi-stat WRS2-SAR images. *International Journal of Applied Earth Observation and Geoinformation* **18**: 69–81. DOI:10.1016/j.jag.2012.01.012.

Gomez B, Phillips JD, Magilligan FJ, James LA. 1997. Floodplain sedimentation and sensitivity: Summer 1993 flood, Upper Mississippi River valley. *Earth Surface Processes and Landforms* **22**: 923–936.

Grenfell M, Aalto R, Nicholas A. 2012. Chute channel dynamics in large, sand-bed meandering rivers. *Earth Surface Processes and Landforms* **37**: 315–331. DOI:10.1002/esp.2257.

Grenfell MC, Nicholas AP, Aalto R. 2014. Mediative adjustment of river dynamics: the role of chute channels in tropical sand-bed meandering rivers. *Sedimentary Geology* **301**: 93–106. DOI:10.1016/j.segeo.2013.006.007.

Gurnell AM, Petts GE, Hannah DM, Smith BPG, Edwards PJ, Kollman J, Ward JV, Tockner K. 2001. Riparian vegetation and island formation along the gravel-bed Fiume Tagliamento, Italy. *Earth Surface Processes and Landforms* **26**: 31–62.

Harrison LR, Dunne T, Fisher GB. 2015. Hydraulic and geomorphic processes in an overbank flood along a meandering, gravel-bed river: implications for chute formation. *Earth Surface Processes and Landforms* **40**: 1239–1253. DOI:10.1002/esp.3717.

Hartley AJ, Weissmann GS, Nichols GJ, Warwick GL. 2010. Large distributive fluvial systems: characteristics, distribution, and controls on development. *Journal of Sedimentary Research* **80**: 167–183.

Hess LL, Melack JM, Novo EMLM, Barbosa CCF, Gastil M. 2003. Dual-season mapping of wetland inundation and vegetation for the central Amazon basin. *Remote Sensing of Environment* **87**: 404–428. DOI:10.1016/j.rse.2003.04.001.

Hickin EJ, Nanson GC. 1975. The character of channel migration on the Beatton River, north-east British Columbia, Canada. *Bulletin of the Geological Society of America* **86**: 487–494.

Hohensinner S, Jungwirth M, Muhar S, Schmutz S. 2014. Importance of multi-dimensional morphodynamics for habitat evolution: Danube River 1715–2006. *Geomorphology* **215**: 3–9. DOI:10.1016/j.geomorph.2013.08.001.

Hudson PF, Sounny-Slitine MA, LaFevor M. 2013. A new longitudinal approach to assess hydrological connectivity: embanked floodplain inundation along lower Mississsippi River. *Hydrological Processes* **27**: 2187–2196. DOI:10.1002/hyp.9838.

James CS. 1985. Sediment transfer to overbank sections. *Journal of Hydraulic Research* **23**: 435–452.

Klasz G, Reckendorfer W, Gabriel H, Baumgartner C, Schmalfuss R, Gutknecht D. 2014. Natural levee formation along a large and regulated river: the Danube in the national Park Donau-Auen, Austria. *Geomorphology*. DOI:10.1016/j.geomorph.2013.12.023.

Kleinhans MG, Ferguson RI, Lane SN, Hardy RJ. 2013. Splitting rivers at their seams: bifurcations and avulsion. *Earth Surface Processes and Landforms* **38**: 47–61. DOI:10.1002/esp.3268.

Kosuth P, Callède J, Laraque A, Filizola N, Guyot JL, Seyler P, Fritsch JM, Guimarães V. 2009. Sea-tide effects on flows in the lower reaches of the Amazon River. *Hydrological Processes* **23**(22): 3141–3150. DOI:10.1002/hyp.7387.

Latrubesse EM. 2008. Patterns of anabranching channels: the ultimate end-member adjustment of mega rivers. *Geomorphology* **101**: 130–145. DOI:10.1016/j.geomorph.2008.05.035.

Latrubesse EM. 2012. Amazon Lakes. In Encyclopedia of Lakes and Reservoirs, Bengtsson L, Herschy RW, Fairbridge RW (eds). Springer: Netherlands; 13–26.

Latrubesse EM. 2015. Large rivers, megafans and other quaternary avulsive fluvial systems: a potential 'who's who' in the geological record. *Earth-Science Reviews* **146**: 1–30. DOI:10.1016/j.earscirev.2015.03.004.

Latrubesse EM, Franzinelli E. 2002. The Holocene alluvial plain of the middle Amazon River, Brazil. *Geomorphology* **44**: 241–257.

Latrubesse EM, Stevaux JC, Sinha R. 2005. Tropical rivers. *Geomorphology* **70**: 187–206.

Lewin J, Ashworth PJ. 2014a. The negative relief of larger floodplains. *Earth-Science Reviews* **129**: 1–23. DOI:10.1016/j.earscirev.2013.10.014.

Lewin J, Ashworth PJ. 2014b. Defining large river channel patterns: alluvial exchange and plurality. *Geomorphology* **215**: 83–98. DOI:10.1016/j.geomorph.2013.02.024.

Lewin J, Hughes D. 1980. Welsh floodplain studies II: application of a qualitative inundation model. *Journal of Hydrology* **46**: 35–49.

Lombardo U. 2016. Alluvial plain dynamics in the southern Amazonian foreland basin. *Earth System Dynamics* **7**: 453–467. DOI:10.5194/esd-7-453-2016.

Mardhiah U, Tillig M, Gurnell A. 2015. Reconstructing the development of sampled sites on fluvial island surfaces of the Tagliamento River, Italy, from historical sources. *Earth Surface Processes and Landforms* **40**: 629–641. DOI:10.1002/esp.3658.

Maurice-Bourgoin L, Martinez J-M, Grelaud J, Filizola N, Boaventura GR. 2005. The role of flood plains in the hydrology and sediment dynamics of the Amazon River, Brazil. *IAHS Publication* **291**: 1–10.

Maurice-Bourgoin L, Bonnet M-P, Martinez J-M, Kosuth P, Cochonneau G, Moreira-Turcq P, Guyot J-L, Vauchel P, Fiozol N, Seyler P. 2007. Temporal dynamics of water and sediment exchanges between the Curuaí floodplain and the Amazon River, Brazil. *Journal of Hydrology* **335**: 140–156. DOI:10.1016/j.hydrol.2006.11.023.

Mertes LAK. 1997. Documentation and significance of the perirheic zone on inundated floodplains. *Water Resources Research* **33**: 1749–1762.

Mertes LAK, Dunne T. 2007. The effects of tectonics, climatic history, and sea-level history on the form and behaviour of the modern Amazon River. In Large Rivers, Gupta A (ed). Wiley: Chichester; 115–144.

Mertes LAK, Dunne T, Martinelli LA. 1996. Channel-floodplain geomorphology along the Solimões -Amazon River, Brazil. *Geological Society of America Bulletin* **108**: 1089–1107. DOI:10.1130/00167606(1996)108<1089:CFGATS>2.3.CO;2.

Middelkoop H. 2000. Heavy-metal pollution of the river Rhine and Meuse floodplains in the Netherlands. *Geologie en Mijnbouw* **79**: 411–428.

Morozova GS. 2005. A review of Holocene avulsions of the Tigris and Euphrates rivers and possible effects on the evolution of civilizations in Lower Mesopotamia. *Geoarchaeology* **20**: 401–423. DOI:10.1002/gea.20057.

Nicholas AP. 2013. Morphological diversity of the world's largest rivers. *Geology* **41**: 475–478. DOI:10.1130/G34016.1.

Nyberg B, Howell JA. 2015. Is the present the key to the past? A global characterization of modern sedimentary basins. *Geology* **43**: 643–646. DOI:10.1130/G36669.1.

O'Brien MP, Wells AT. 1986. A small alluvial crevasse splay. *Journal of Sedimentary Petrology* **56**: 876–879.

Olariu C, Bhattacharya JP, Leybourne MI, Boss SK, Stern RJ. 2012. Interplay between river discharge and topography of the basin floor in a hyperpyncnal lacustrine basin. *Sedimentology* **59**: 704–728.

Park E, Latrubesse EM. 2015. Modelling suspended sediment distribution patterns of the Amazon River using MODIS data. *Remote Sensing of Environment* **147**: 232–242. DOI:10.1016/j.rse.2014.03.013.

Paira AR, Drago EC. 2007. Origin, evolution, and types of floodplain water bodies. In The Middle Paraná River, Iriondo MH, Paggi JC, Parma MJ (eds). Springer-Verlag: Berlin; 53–81.

Pizzuto JE. 1987. Sediment diffusion during overbank flows. *Sedimentology* **34**: 301–317.

Richey JE, Mertes LAK, Dunne T, Victoria RL, Forsberg BR, Tancredi ACNS, Oliveira E. 1989. Sources and routing of the Amazon River flood wave. *Global Biogeochemical Cycles* **3**: 191–204. DOI:10.1029/GB003i003p00191.

Ritter DF. 1975. Stratigraphic implications of coarse-grained gravel deposited as overbank sediment, Southern Illinois. *The Journal of Geology* **83**(5): 645–650.

Rowland JC, Dietrich WE, Day G, Parker G. 2009. Formation and maintenance of single-thread tie channels entering floodplain lakes: observations from three diverse river systems. *Journal of Geophysical Research* **114**: 1–18. DOI:10.1029/2008JF001073.F02013.

Rowland JC, Dietrich WE, Stacey MT. 2010. Morphodynamics of subaqueous levee formation: insights into river mouth morphologies arising from experiments. *Journal of Geophysical Research* **115**: 1–20. DOI:10.1029/2010JF001684.F04007.

Rowland JC, Lepper K, Dietrich WE, Wilson CJ, Sheldon R. 2005. Tie channel sedimentation rates, oxbow formation age and channel migration rate from optically stimulated luminescence (OSL) analysis of floodplain deposits. *Earth Surface Processes and Landforms* **30**: 1161–1179. DOI:10.1002/esp.1268.

Rozo MG, Nogueira ACR, Castro CS. 2014. Remote sensing-based analysis of the planform changes in the Upper Amazon river over the period 1986–2006. *Journal of South American Earth Sciences* **51**: 28–44. DOI:10.1016/j.sames.2013.12.004.

Rozo MG, Nogueira ACR, Truckenbrodt W. 2012. The anastomosing pattern and the extensively distributed scroll bars in the middle Amazon River. *Earth Surface Processes and Landforms* **14**: 1471–1488. DOI:10.1002/esp.3249.

Rudorff CM, Melack JM, Bates PD. 2014. Flooding dynamics on the lower Amazon floodplain: 1. Hydraulic controls on water elevation, inundation extent and river-floodplain discharge. *Water Resources Research* **50**: 619–634. DOI:10.1002/2013WR014091.

Saucier RT. 1994. Geomorphology and Quaternary Geologic History of the Lower Mississippi Valley. Mississippi River Commission: Vicksburg.

Schuurman F, Marra WA, Kleinhans MG. 2013. Physics-based modeling of large braided sand-bed rivers: bar pattern formation, dynamics, and sensitivity. *Journal of Geophysical Research - Earth Surface* **118**: 1–19. DOI:10.1002/2013JF002896

Schwendel AC, Nicholas AP, Aalto RE, Sambrook Smith GH, Buckley S. 2015. Interaction between meander dynamics and floodplain heterogeneity in a large tropical sand-bed river. *Earth Surface Processes and Landforms* **40**: 2026–2040. DOI:10.1002/esp.3777.

Scown MW, Thoms MC, De Jager NR. 2015. Floodplain complexity and surface metrics: influences of scale and geomorphology. *Geomorphology*. DOI:10.1016/j.geomorph.2015.05.024.

Shen Z, Törnqvist TE, Mauz B, Chamberlain EL, Nijhuis AG, Sandoval L. 2015. Episodic overbank deposition as a dominant mechanism of floodplain and delta-plain aggradation. *Geology* **43**: 875–878. DOI:10.1130/G36847.1.

Skonieczny C, Paillou P, Bory A, Bayon G, Biscara L, Crosta X, Eynaud F, Malaize B, Revel M, Aleman N, Barusseau J-P, Vernet R, Lopez S, Grousset F. 2015. African humid periods triggered the reactivation of a large river system in Western Sahara. *Nature Communications* **6**: 8751. DOI:10.1038/ncomms9751.

Slingerland R, Smith ND. 2004. River avulsions and their deposits. *Annual Review of Earth and Planetary Sciences* **32**: 257–285. DOI:10.1146/annurev.earth.32.101802.120201.

Smith DG. 1986. Anastomosing river deposits, sedimentation rates and basin subsidence, Magdalena River, Northwestern Columbia, South America. *Sedimentary Geology* **46**: 177–196.

Smith ND, Pérez-Arlucea M. 1994. Fine-grained splay deposits in the avulsion belt of the lower Saskatchewan River, Canada. *Journal of Sedimentary Research* **B64**: 159–168.

Smith ND, Cross TA, Dufficy JP, Clough SR. 1989. The anatomy of an avulsion. *Sedimentology* **36**: 1–23.

Syvitski JPM, Brackenridge GR. 2013. Causation and avoidance of catastrophic flooding along the Indus River, Pakistan. *GSA Today* **23**: 4–10. DOI:10.1130/GSATG165A.1.

Syvitski JPM, Kettner AJ. 2011. Sediment flux and the Anthropocene. *Philosophical Transactions of the Royal Society A* **369**: 957–975. DOI:10.1098/rsta.2010.0329.

Syvitski JPM, Overeem I, Brackenridge GR, Hannon M. 2012. Floods, floodplains, delta plains – a satellite imaging approach. *Sedimentary Geology* **267–268**: 1–14. DOI:10.1016/j.sedgeo.2012.05.014.

Thorne CR, Russell APG, Alam MK. 1993. Planform pattern and channel evolution of the Brahmaputra River, Bangladesh. In Braided Rivers, Best JL, Bristow CS (eds), Vol. **75**. Special Publication of the Geological Society of London: London; 257–276.

Toonen WHJ, Kleinhans MG, Cohen KM. 2012. Sedimentary architecture of abandoned channel fills. *Earth Surface Processes and Landforms* **37**: 459–472. DOI:10.1002/esp.3189.

Toonen WHJ, van Asselen S, Stouthamer E, Smith ND. 2016. Depositional development of the Muskeg Lake crevasse splay in the Cumberland Marshes (Canada). *Earth Surface Processes and Landforms* **41**: 117–129. DOI:10.1002/esp.3791.

Tooth S. 1999. Floodouts in central Australia. In Varieties of Fluvial Form, Miller AJ, Gupta S (eds). Wiley: Chichester; 219–247.

Tooth S. 2005. Splay formation along the lower reaches of ephemeral rivers on the Northern Plains of arid central Australia. *Journal of Sedimentary Research* **75**: 634–647.

Tooth S, McCarthy TS. 2007. Wetlands in drylands: geomorphological and sedimentological characteristics, with emphasis on examples from southern Africa. *Progress in Physical Geography* **31**: 3–41.

Törnqvist TE, Bridge JS. 2002. Spatial variation of overbank aggradation rate and its influence on avulsion frequency. *Sedimentology* **49**: 891–905.

Tricart JF. 1977. Types de lits fluviaux en Amazonie brésilienne. *Annales de Géographie* **86**: 1–54. DOI:10.3406/geo.1977.17567.

Trigg MA, Bates PD, Wilson MD, Schumann G, Baugh C. 2012. Floodplain channel morphology and networks of the middle Amazon River. *Water Resources Research* **48** . DOI:10.1029/2012WR01188. W10504

Tye RS, Coleman JM. 1989. Depositional processes and stratigraphy of fluvially dominated lacustrine deltas: Mississippi delta plain. *Journal of Sedimentary Petrology* **59**: 973–996.

van de Lageweg WI, Van Dyke WM, Kleinhans MG. 2013. Morphological and stratigraphical signatures of floods in braided gravel-bed river revealed from flume experiments. *Journal of Sedimentary Research* **83**: 1032–1045. DOI:10.2110/jsr.2013.70.

Weissmann GS, Hartley AJ, Nichols GJ, Scuderi LA, Olson M, Buehler H, Banteah R. 2010. Fluvial form in modern continental sedimentary basins: distributive fluvial systems. *Geology* **38**: 39–42.

Weissmann GS, Hartley AJ, Scuderi LA, Nichols GJ, Owen A, Wright A, Felicia AL, Holland F, Anaya FML. 2015. Fluvial geomorphic elements in modern sedimentary basins and their potential preservation in the rock record: a review. *Geomorphology* **250**: 187–219. DOI:10.1016/j.geomorph.2015.09.005.

Wheaton JM, Fryirs KA, Brierley G, Bangen SG, Bouwes N, O'Brien G. 2015. Geomorphic mapping and taxonomy of fluvial landforms. *Geomorphology* **248**: 273–295. DOI:10.1016/j.geomorph.2015.07.010.

Wintenberger CL, Rodrigues S, Bréhéret J-G, Villar M. 2015. Fluvial islands: first stage of development from non-migrating (forced) bars and woody-vegetation interactions. *Geomorphology* **246**: 305–320. DOI:10.1016/j.geomorph.2015.06.026.

Wood SH, Ziegler AD, Bundarnsin T. 2008. Floodplain deposits, channel changes and riverbank stratigraphy of the Mekong River area at the 14th century city of Chiang Saen, Northern Thailand. *Geomorphology* **101**: 510–523. DOI:10.1016/j.geomorph.2007.04.030.

Zinger JA, Rhoads BL, Best JL. 2011. Extreme sediment pulse generated by bend cutoffs along a large meandering river. *Nature Geoscience* **4**: 675–678. DOI:10.1038/NGEO1260.

Zhuang Y, Kidder TR. 2014. Archaeology of the Anthropocene in the Yellow River region, China 8000–2000 cal. BP. *The Holocene* **24**: 1602–1623. DOI:10.1177/0959683614544058.

